PCCP

PAPER

View Article Online
View Journal | View Issue



Cite this: *Phys. Chem. Chem. Phys.*, 2023, **25**, 13376

# Scaling of the permanent electric dipole moment in isolated silicon clusters with near-spherical shape†

Filip Rivic, * Andreas Lehr and Rolf Schäfer

Received 28th February 2023,
Accepted 21st April 2023

DOI: 10.1039/d3cp00926b

rsc.li/pccp

In silicon clusters a structural transition from prolate to near-spherical structures takes place at a size of about 25–30 atoms. While some of the prolate clusters are very polar, there has been no experimental evidence of the presence of dipole moments in larger silicon clusters with near-spherical shape. By means of electric molecular beam deflection experiments at cryogenic temperatures, it was possible to prove for the first time that $Si_N$ clusters with more than $N$ = 30 atoms are also polar. Interestingly, the dipole moment per atom for clusters in the range between 30 and 80 or 90 atoms is almost constant and amounts to 0.02 D. This unusual behaviour manifests in effective polarizabilities increasing linearly with cluster size. The dipolar contribution to the polarizability means that $Si_N$ clusters with $N$ = 80 atoms can be polarized more than twice as well as a correspondingly small sphere with the dielectric properties of bulk α-Si. This finding is analysed with quantum chemical calculations concerning the geometric structure as well as the charge distribution and is related to the dielectric behaviour of polar semiconductor nanocrystals.



## 1. Introduction

Although Si nanostructures have many potential applications in nanoelectronics,[1–3] the dielectric behaviour of Si clusters has not been sufficiently investigated and understood. In an older work, there was an indication that in $Si_N$ clusters with $N$ = 60–120 atoms, the dielectric constant is lowered as a consequence of the quantum confinement compared to the bulk material.[4] For this purpose, electric beam deflection experiments were carried out. From the deflection of the clusters by an inhomogeneous electric field, the polarizability α was determined and converted into the dielectric constant with the help of the Clausius–Mossotti relationship.[5] In a more recent work,[6] this effect could not be confirmed, since the values for the polarizabilities were found to agree well with those of a small polarizable sphere with the dielectric properties of bulk α-Si.[7] However, the experiments were performed on thermally excited clusters, for which a possible dipolar contribution is almost completely quenched and therefore hardly observable.[8] In this work, we now present for the first time electric molecular beam deflection experiments at cryogenic temperatures so that the nanoclusters are rigid to a good approximation.[9] With this, it was possible to demonstrate that $Si_N$ clusters are polar in the range between 30–80 or 90 atoms. At first glance, this finding is somewhat unusual because $Si_N$ clusters form compact, nearly spherical structures in this size range. The detection of permanent electric dipole moments $\mu$ is equivalent to the fact that the Si atoms in the clusters are permanently polarised, *i.e.* carry partial charges. Obviously, the chemical bonding between the Si atoms in the clusters differs from bulk Si. In connection with quantum chemical calculations and in comparison with the dielectric behaviour of II–VI semiconductor nanoparticles, the physical cause of the observation is discussed.

## 2. Experiment

The experimental setup has already been described in detail in the literature.[10] In contrast to the electric beam deflection measurements at room temperature,[6] a cluster source with a nozzle is used for the experiments shown here, which is cooled to $T_{nozzle}$ = 16 K with the help of a closed-cycle cryostat.[11,12] Since the lowest vibrational modes (*cf.* ESI†) are not considerably thermally excited at 16 K, this ensures that the clusters can

*Technical University of Darmstadt, Eduard-Zintl-Institute, Alarich-Weiss-Straße 8, 64287 Darmstadt, Germany. E-mail: filip.rivic@tu-darmstadt.de*

† Electronic supplementary information (ESI) available: Mass spectrum of $Si_N$ clusters; electric beam deflection profiles for selected clusters; experimentally deduced dipole moments and effective polarizabilities with uncertainties; calculated dipole moments and electronic polarizabilities of $Si_{30}$ employing various exchange-correlation functionals; Cartesian coordinates and Mulliken partial charges of selected clusters; lowest vibrational modes of selected clusters. See DOI: https://doi.org/10.1039/d3cp00926b

be regarded as rigid rotors to a good approximation. In contrast, at a nozzle temperature of 300 K, it is expected that the clusters are strongly vibrationally excited, *i.e.* these clusters are floppy and the electric dipole moment is completely quenched.[5] In total, two series of measurements are presented that were performed with different helium valve opening times and hence at different cluster generation conditions. Due to this changed setting, the cluster velocities are different in both measurements, although the nozzle temperatures were the same. In the first series of measurements, the velocity of the clusters with $N$ = 30–80 was (640 ± 20) m s$^{-1}$, while in the second measurement the clusters were about 100 m s$^{-1}$ faster. In the second measurement, the intensities of the clusters are higher, so that the corresponding data are characterised by a better signal-to-noise ratio. Therefore, it was possible to study clusters in the range $N$ = 30–90. However, the higher cluster velocities indicate that these clusters are more rotationally excited, *i.e.* the ensemble of clusters in the second measurement is characterised by a larger value of the rotational temperature.[12] The first measurement was carried out with a deflection voltage of $U$ = 11 kV (electric field strength $E = 7 \times 10^6$ V m$^{-1}$), while in the second measurement $U$ = 30 kV ($E = 2 \times 10^7$ V m$^{-1}$) were applied to the electrodes.

For the evaluation of the electric deflection profiles (*cf.* ESI† for details), it should be noted that the rotational energy and the interaction energy of the electric dipole with the external electric field is nearly the same for very polar structures, at least for a deflection voltage of $U$ = 30 kV. Thus, an evaluation of the beam deflection profiles in order to determine the electric dipole moment $\mu$ is, strictly speaking, no longer justified within the framework of the first-order perturbation theory (FOPT).[13] In addition, the application of FOPT presupposes that the clusters are approximately spherical rotors. This, too, is not necessarily ensured *a priori*. Nevertheless, the beam profiles were evaluated based on the FOPT because, on the one hand, this means that no structural information is necessary for the analysis and, on the other hand, deviations from the spherical geometry usually have an effect of significantly less than 20% on the determination of the dipole moments, especially for near-spherical shaped clusters.[13] Furthermore, this procedure is by far the most effective, since only the broadening of the beam profile due to the inhomogeneous field has to be determined to extract the electric dipole moment $\mu$ with

$$\frac{\mu}{N} = 3\frac{\sqrt{\langle b_{\mathrm{on}}{}^2\rangle - \langle b_{\mathrm{off}}{}^2\rangle}}{N} \qquad (1)$$

where $\langle b^2\rangle$ is the variance in Debye of a Gaussian function fitted to the experimental beam defection profile with (on) and without (off) electric field.[8] In particular, this procedure is justified for the fundamental clarification of the question of whether the investigated $Si_N$ clusters are polar or not. The broadening is determined by fitting a Gaussian function to the beam deflection profile without and with electric field. The effective polarizability $\alpha_{\mathrm{eff}}$ is obtained from the shift of the beam profile when the electric field is applied. For the analysis of $\alpha_{\mathrm{eff}}$, however, it is mandatory to apply the second-order perturbation theory (SOPT)[13–15]

$$\frac{\alpha_{\mathrm{eff}}}{N} = \frac{\alpha_{\mathrm{el}}}{N} + \frac{2}{9}\frac{\left(\frac{\mu}{N}\right)^2}{k_{\mathrm{B}}T_{\mathrm{Rot}}}N, \qquad (2)$$

since in the case of polar clusters the dipolar contribution can outweigh the intrinsic electronic contribution $\alpha_{\mathrm{el}}$ to the polarizability. Strictly speaking, this relationship only applies to spherical rotors. For the estimation of the dipolar contribution, *i.e.* the second term, values of the rotational temperature $T_{\mathrm{Rot}}$ and the permanent electric dipole moment $\mu$ of the clusters are necessary.

## 3. Results

The dependency of the electric dipole moment $\mu$ and the effective polarizability $\alpha_{\mathrm{eff}}$ on the cluster size $N$ is shown in Fig. 1 for the two measurements. For this purpose, the values of the permanent electric dipole moment per atom $\mu/N$ and of the polarizability per atom $\alpha_{\mathrm{eff}}/N$ are plotted against the size of the clusters. It can be clearly seen that the $Si_N$ clusters in the investigated size range of 30–80 or 90 atoms are polar and have an approximately size-independent dipole moment per atom, *i.e.* the total dipole moment $\mu$ increases approximately linearly with cluster size $N$. The value of the determined dipole moment per atom of $\mu/N = (2.00 \pm 0.04) \times 10^{-2}$ D is approximately the same in both measurements. This finding indicates that the clusters in both measurements can be regarded as rigid rotors regardless of their different velocities. If in the second measurement with higher velocities and stronger rotational excitation the clusters were already vibrationally excited, one would expect that the electric dipole moment would already be partially quenched, *i.e.* the beam broadening would be reduced and lower values of the dipole moment would be observed.[8] Since the dipolar contribution to the effective polarizability depends on the square of the permanent dipole moment, a linear increase in the effective polarizability per atom $\alpha_{\mathrm{eff}}/N$ with the cluster size $N$ is observed. However, the increase in polarizability is different in the two measurements. In the first measurement, the change in the effective polarizability per atom with the cluster size is equal to (0.11 ± 0.02) Å$^3$, while in the second measurement a value of (0.06 ± 0.01) Å$^3$ is observed. This difference results from a different degree of rotational excitation of the clusters in the two measurements. If one uses the values of the dipole moment of $\mu/N = (2.00 \pm 0.04) \times 10^{-2}$ D obtained from the beam broadening using the FOPT, one obtains a value for the rotational temperature of (6 ± 1) K in the first measurement and (11 ± 2) K in the second measurement according to eqn (2). These two values for the rotational temperature appear realistic for the measured cluster velocities.[12] Also plotted in Fig. 1 is the value of the polarizability per atom of 3.71 Å$^3$ expected for a small sphere with the dielectric properties of bulk α-Si according to the Clausius–Mossotti relationship.[5,7] It can be seen that the effective polarizabilities of the smallest here investigated clusters with 30 atoms are similar to those expected for a small sphere with

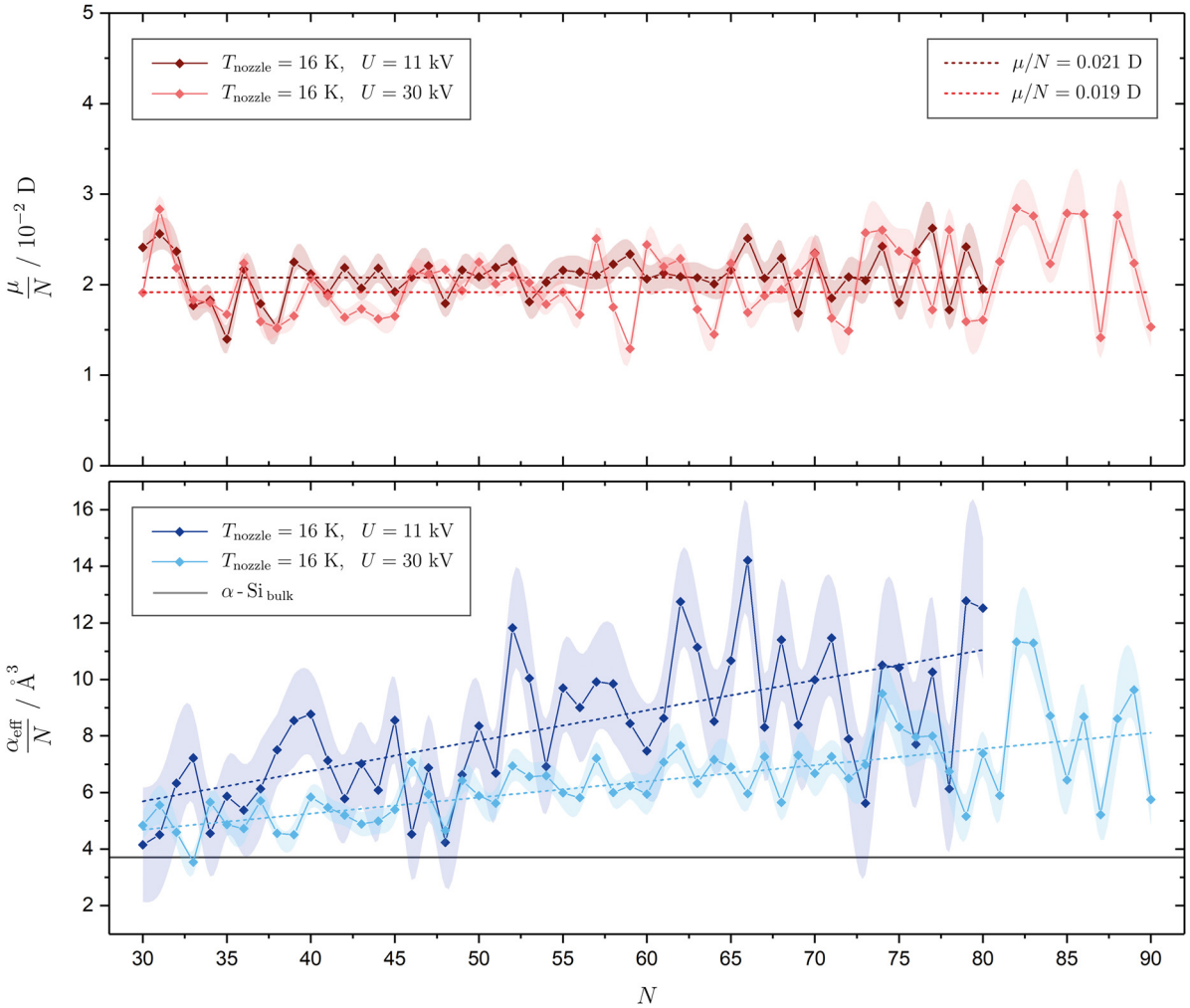


Fig. 1 Permanent electric dipole moments per atom $\mu/N$ (top) and effective polarizabilities per atom $\alpha_{eff}/N$ (bottom) obtained from electric molecular beam deflection experiments at $T_{nozzle}$ = 16 K and deflection voltages of $U$ = 11 kV and 30 kV for $Si_N$ clusters with $N$ = 30–80 or 90. Experimental uncertainties are displayed as continuous error functions. Linear fits to guide the eye are shown as dashed lines; for the dipole moment per atom the slope is set to zero and an average dipole moment per atom of (0.020 ± 0.04) D is determined. The bulk α-Si polarizability per atom of 3.71 Å$^3$ is estimated from the Clausius–Mossotti relationship and is shown as gray horizontal line.[5,7]

the bulk properties of α-Si within the limits of measurement accuracy. Thus, the dipolar contribution plays almost no role here. However, the dipolar contribution to the effective polarizability of the largest clusters investigated here is comparable to the intrinsic electronic polarizability, so that these clusters are more than twice as polarisable as a correspondingly small sphere with the dielectric properties of α-Si.

## 4. Quantum chemistry

Quantum chemical calculations were carried out to interpret the observed behaviour. To analyse the dielectric response of the $Si_N$ clusters, structures of the clusters found in the literature[16] were adopted and locally reoptimised. For this purpose, density functional theory (DFT) was applied employing the hybrid exchange–correlation functional PBE0[17] together with the cc-pVTZ basis set.[18] This level of theory has been chosen because it has led to good results in the description of tetrel clusters in the past.[19,20] However, it should be noted that the starting structures used do not necessarily belong to the global minimum. Performing a global optimisation for the investigated $Si_N$ clusters would be possible in principle, but enormously time and resource consuming for the larger clusters under study at the DFT level of theory. Even if the locally optimized structures do not exactly match the structures of the clusters in the experiment, one can still expect to see a trend regarding the size dependence of the dielectric properties.

Table 1 shows the calculated dipole moments per atom together with the experimental values from the two measurements. It can be seen well that also the theoretically predicted dipole moments per atom are approximately independent of the cluster size, *i.e.* also theoretically it is observed that all clusters are polar and the dipole moment increases linearly with the cluster size to a good approximation. However, the calculated values of the dipole moment are about twice as large

 

Table 1 Calculated and experimental electric permanent dipole moments and polarizabilities per atom $\mu/N$ and $\alpha_{el}/N$ as well as $\alpha_{eff}/N$ of $Si_N$ clusters with $N$ = 30, 35, 40, 45, 50, 55, 60, 70 and 80. Values of the experimental uncertainties can be found in the ESI†

| | Simulation | | Experiment (11 kV) | | Experiment (30 kV) | |
|---|---|---|---|---|---|---|
| $N$ | $\frac{\mu}{N}/10^{-2}$ D | $\frac{\alpha_{el}}{N}$/Å$^3$ | $\frac{\mu}{N}/10^{-2}$ D | $\frac{\alpha_{eff}}{N}$/Å$^3$ | $\frac{\mu}{N}/10^{-2}$ D | $\frac{\alpha_{eff}}{N}$/Å$^3$ |
| 30 | 3.80 | 4.35 | 2.41 | 4.15 | 1.91 | 4.84 |
| 35 | 4.98 | 4.31 | 1.40 | 5.87 | 1.67 | 4.86 |
| 40 | 3.02 | 4.30 | 2.12 | 8.77 | 2.07 | 5.84 |
| 45 | 6.82 | 4.20 | 1.92 | 8.55 | 1.65 | 5.40 |
| 50 | 4.34 | 4.32 | 2.09 | 8.35 | 2.25 | 5.89 |
| 55 | 4.31 | 4.33 | 2.16 | 9.70 | 1.92 | 5.99 |
| 60 | 4.11 | 4.24 | 2.06 | 7.46 | 2.44 | 5.94 |
| 70 | 4.95 | 4.34 | 2.35 | 9.98 | 2.34 | 6.67 |
| 80 | 3.43 | 4.35 | 1.95 | 12.53 | 1.61 | 7.38 |

than found in the experiment. This can have various causes: In order to capture the influence of the exchange–correlation functional employed, different hybrid functionals were used for $Si_{30}$ (*cf.* ESI† for details). For this purpose, a local geometry optimisation was carried out in each case. It is demonstrated that the computed value of the dipole moment can change by 30% to give a lower bound close to the experimental value, whereas values up to almost three times as high compared to the experimental value can be obtained depending on the functional in use. From an experimental point of view, it must be noted that the beam profile broadenings, *i.e.* the determination of $\mu$, were evaluated according to the FOPT and therefore deviations from the spherical geometry are not taken into account.‡ [13]

Since very similar values for the dipole moment were obtained at $U$ = 11 kV and 30 kV, the influence of the electric field strength seems to be negligible. It should be noted, however, that although the experiments were carried out in high vacuum at a base pressure of $4 \times 10^{-7}$ mbar, ensuring a mean free path of the clusters being significantly larger than the dimensions of the apparatus, the background gas can still have an impact on the rotational dynamics.[21] This can be important, especially in the case of asymmetric rotors, and lead to the beam broadening being partially quenched. Thus, lower values of the dipole moment are obtained. However, despite the discrepancies in the absolute value, the trend that the dipole moment per atom is approximately constant is theoretically correctly reproduced.

## 5. Discussion

In order to better understand the cause of the increasing polarity of the $Si_N$ clusters with the cluster size, a population analysis was carried out and partial (net atomic) charges $\delta q$ were calculated according to Mulliken.[22] However, one has to take into account that the calculated dipole moments $\mu$ based on the Mulliken atomic charges does not necessarily fit to the predicted values shown in Table 1.[23] Even though the decomposition of the wave function is not unambiguous, this gives a first insight to the partial charge distribution in the clusters. The reoptimised structures of the clusters are shown in Fig. 2 oriented along their dipole moments $\mu$ displayed as an arrow with partial charges $\delta q$ indicated by a colour code (blue: negative, red: positive partial charge). It can be clearly seen that there are areas in the clusters with a positive or negative excess charge. It seems that, starting from the centre of the cluster, a strongly negatively charged cluster core is formed, which is surrounded by a shell of positively charged Si atoms. As the cluster size increases, there are also more and more Si atoms on the cluster surface, which are slightly negatively charged. As the clusters grow, the amount of charges contained in the negatively charge core and the positively charge shell increase. Therefore, the electric dipole moment increases as well.

In order to quantify this effect, the centres of positive and negative charge have been localised and the sum of positive partial charges $\delta q^{(+)}$ contained in these centres has been calculated based on the Mulliken partial charges. These values are given in Table 2. To see how the sum of positive partial charges $\delta q i^{(+)}$ contained in these centres changes with cluster size $N$, a double-logarithmic plot is shown in Fig. 3. This demonstrates that the sum of positive partial charges increases approximately linear with $N^{2/3}$, which is proportional to the surface area of the cluster. Interestingly, the electric dipole moment per atom calculated from the partial charges is also almost independent of size, except for $N$ = 45 and 60. The reason for the asymmetric charge distribution is that the structures of the clusters do not represent a cut-out of the bulk silicon structure. Due to the free surface, the cluster tries to minimise its energy by forming different coordination geometries locally around each Si atom.[25–28] The resulting structures therefore rather resemble structural sections from amorphous than from crystalline silicon.[29]

To quantify the differences in the coordination sphere, coordination numbers (CNs) were calculated using a tolerance criterion. All atoms within a sphere around a selected atom are counted as part of the coordination sphere. The tolerance criterion for the radius of this sphere was 1.1$d$, where $d$ is the bond distance between two Si atoms in α-Si of 2.352 Å.[24] Table 2 now shows CNs calculated in this way for Si atoms in the core and the shell of the clusters. The outer bound of the cluster shell is defined by the most distant Si atom relative to the centre of mass and has a thickness of 0.5$d$, *i.e.* $N_{shell}$ gives the number of Si atoms in that shell. It can be clearly seen that the negatively charged Si atoms in the cluster core have significantly larger CNs than the positively charged atoms in the shell surrounding them. As a result, the chemical bonding between atoms in the cluster core and the surrounding shell becomes polar, resulting in a non-vanishing electric dipole

‡ It is shown for the $Ge_{15}$ cluster which is assumed to have a very prolate geometric structure[13] that the dipole moment obtained by the FOPT approach used in our work deviates only about 16% from the one obtained by quantum chemical calculations and confirmed by classical trajectory simulations. For the clusters discussed in this work, the deviation from the spherical shape is much smaller so that the difference between the electric dipole moments is assumed to be smaller as well.

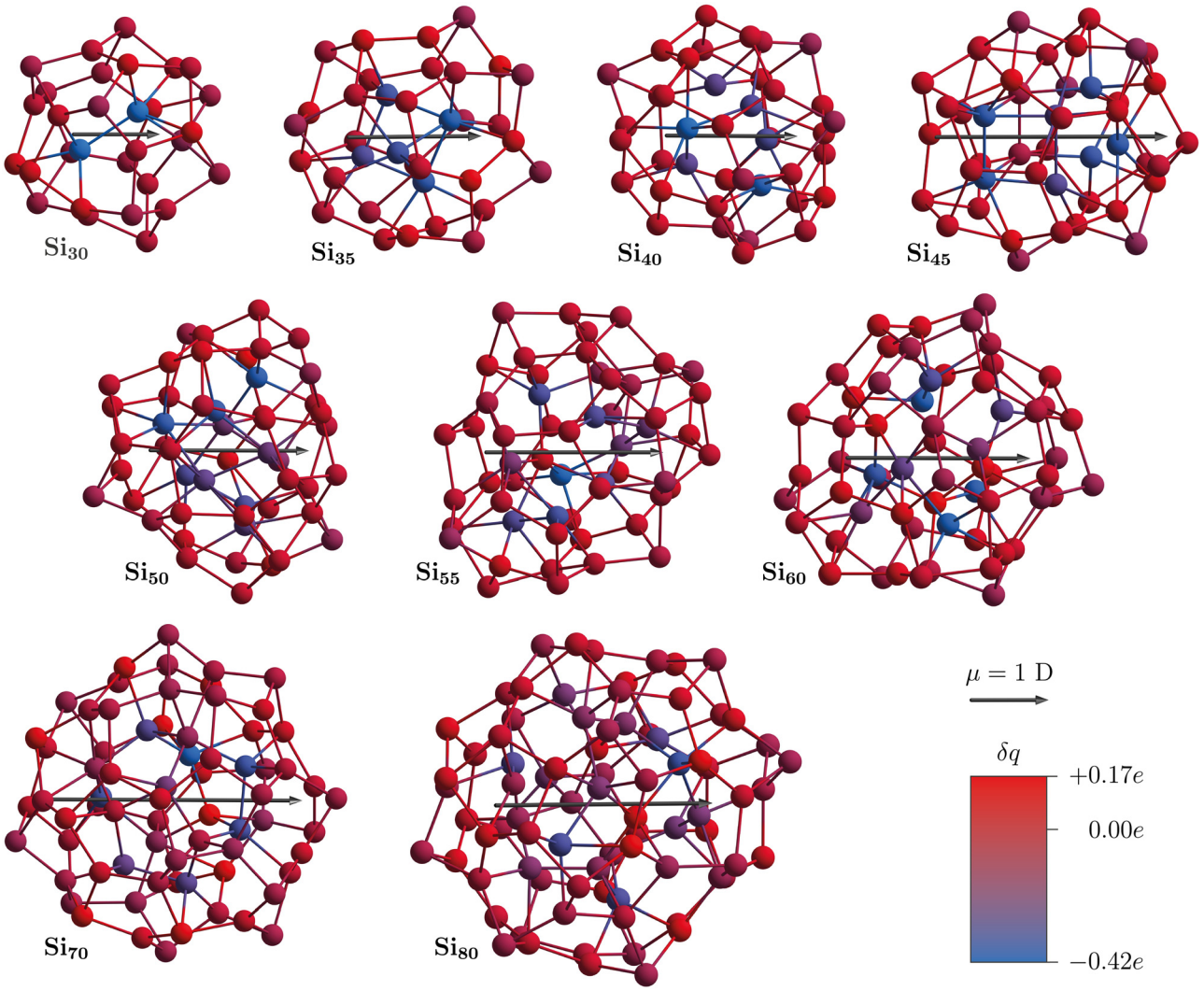


Fig. 2 Geometric structures of $Si_N$ clusters with $N$ = 30, 35, 40, 45, 50, 55, 60, 70 and 80 reoptimised at the PBE0/cc-pVTZ level of theory. The clusters are oriented around their computed permanent dipole moments $\mu$ shown as vectors with absolute values given by the length of the vector (*cf.* Table 1 for details). Mulliken partial charges $\delta$ are indicated by a colour code ranging from positive (red) to negative (blue) partial charges (*cf.* ESI† for details).

Table 2 Sum of positive partial charges $\delta q^{(+)}$, number of core and shell atoms $N_{core}$ and $N_{shell}$ for the calculated $Si_N$ clusters with $N$ = 30, 35, 40, 45, 50, 55, 60, 70 and 80 together with their corresponding average coordination numbers CN calculated *via* a tolerance criterion of 1.1$d$ where $d$ = 2.352 Å is the Si–Si bond distance in bulk α-Si.[24]

| $N$ | $\sum_{i=1}^{N} \delta q_i^{(+)}$ | $N_{core}$ | $CN_{core}$ | $N_{shell}$ | $CN_{shell}$ |
|---|---|---|---|---|---|
| 30 | 0.96 | 2 | 4.50 | 28 | 3.32 |
| 35 | 1.45 | 7 | 5.14 | 28 | 3.50 |
| 40 | 1.64 | 7 | 4.43 | 33 | 3.73 |
| 45 | 2.03 | 11 | 5.27 | 34 | 4.06 |
| 50 | 2.10 | 9 | 5.56 | 41 | 4.02 |
| 55 | 2.01 | 13 | 4.46 | 42 | 3.81 |
| 60 | 2.28 | 10 | 5.90 | 50 | 3.70 |
| 70 | 2.26 | 18 | 4.22 | 52 | 3.42 |
| 80 | 2.52 | 19 | 4.21 | 61 | 3.67 |

moment that increases with the cluster size. The fact that the coordination numbers of Si atoms in the cluster core are significantly increased compared to atoms in the surrounding shell has already been shown in a whole series of theoretical papers.[25–28] Here, it is pointed out how the individually different coordination geometry around each Si atom affects the total dipole moment of the $Si_N$ clusters.

A similar behaviour has already been observed in semiconductor nanocrystals (NCs).[30] For example, in polar CdSe nanorods, it was observed that the dipole moment increases linearly with the volume.[31] This was attributed to the naturally existing polar character of the present wurtzite structure. Other approaches point to structural deviations from the ideal wurtzite type as the cause of the presence of the dipole moment.[32] Interestingly, permanent electric dipole moments are also observed in ZnSe nanostructures of the zinc blende type, which increase with the diameter of the NC.[33] In a subsequent study, it was shown that small deviations from the symmetric-tetrahedral shape are responsible for the dipole moments.[34] Accordingly, even PbSe-NCs with a centrosymmetric crystal

 

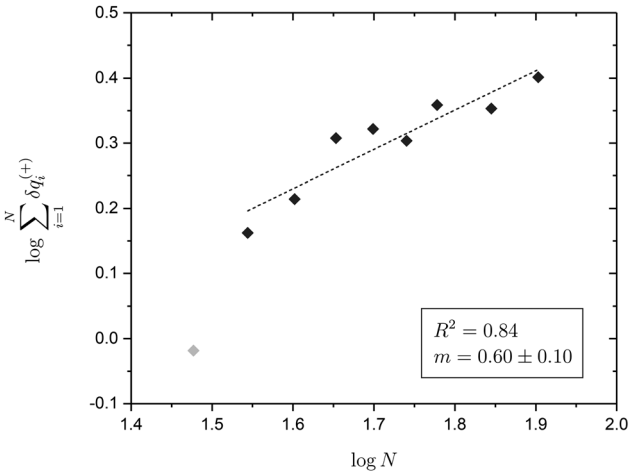


Fig. 3 Double-logarithmic presentation of the sum of positive partial charges $\delta q^{(+)}$ as a function of the amount of atoms $N$ in the cluster. When omitting the value of the lightly more prolate $Si_{30}$ cluster, a slope $m$ of approximately 2/3 with a coefficient of determination of $R^2$ = 0.84 is obtained.

lattice can be polar.[35] How the coordination number affects the partial charge of the atoms has been shown for InP nanoclusters.[36] Deviations of the arrangement of atoms on the surface from the ideal tretrahedral structure leads to the appearance of dipole moments in nanocrystals with a cubic crystal lattice.[35] In the case of the NCs, the reconstruction of the structure due to the presence of the free surface causes the formation of electric dipole moments, which is very similar to the Si clusters. Correspondingly, the dipole moment density, *i.e.* the dipole moment related to the volume, for the $Si_N$ clusters examined here is with an experimental value of $(0.30 \pm 0.01)$ μC cm$^{-2}$ in a similar range of values to that observed for the CdSe nanocrystals.[31,32] Interestingly, hydrogenated Si-NCs also show dipole moments, which are important for the controlled assembly of silicon-based nanostructures.[37] With the work presented here, it is now additionally shown that isolated $Si_N$ nanoclusters in the gas phase are also polar despite their compact, near-spherical shape.

## 6. Summary

In the present work, the dielectric properties of near-spherical silicon clusters in the size range between 30 and 90 atoms were investigated under cryogenic conditions for the first time. This clearly demonstrated that the investigated $Si_N$ clusters are polar and that the dipole moment per atom is almost constant. This leads to the effective polarizability of the clusters increasing linearly with the cluster size. The electric dipole moment results from the structural shape of the cluster: in a surrounding shell a core of Si atoms is located with significantly higher coordination numbers. This asymmetry leads to a polar chemical bonding between the Si atoms and ultimately to the formation of a permanent electric dipole moment.

## Conflicts of interest

There are no conflicts to declare.

## Acknowledgements

Financial support for this project was provided by the Deutsche Forschungsgemeinschaft (Grant SCHA 885/15-2). The authors gratefully acknowledge the computing time provided to them on the high-performance computer Lichtenberg at the NHR Centers NHR4CES at TU Darmstadt. We would like to thank Koblar A. Jackson regarding discussions on silicon cluster dipole moments.

## References

1 D. Hiller, R. Duffy, S. Strehle and P. Stradins, *Phys. Status Solidi*, 2020, **217**, 2000023.
2 N. Koshida, *Device Applications of Silicon Nanocrystals and Nanostructures*, Springer US, 2009.
3 M. Nayfeh, *Fundamentals and Applications of Nano Silicon in Plasmonics and Fullerines*, Elsevier, 2018.
4 R. Schäfer, S. Schlecht, J. Woenckhaus and J. A. Becker, *Phys. Rev. Lett.*, 1996, **76**, 471–474.
5 S. Heiles and R. Schäfer, *Dielectric Properties of Isolated Clusters: Beam Deflection Studies*, Springer, 2014.
6 D. A. Götz, S. Heiles and R. Schäfer, *Eur. Phys. J. D*, 2012, **66**, 293.
7 L.-W. Wang and A. Zunger, *Phys. Rev. Lett.*, 1994, **73**, 1039–1042.
8 S. Schäfer, B. Assadollahzadeh, M. Mehring, P. Schwerdtfeger and R. Schäfer, *J. Phys. Chem. A*, 2008, **112**, 12312–12319.
9 D. A. Götz, S. Heiles, R. L. Johnston and R. Schäfer, *J. Chem. Phys.*, 2012, **136**, 29–31.
10 S. Schäfer, M. Mehring, R. Schäfer and P. Schwerdtfeger, *Phys. Rev. A: At., Mol., Opt. Phys.*, 2007, **76**, 052515.
11 U. Rohrmann, P. Schwerdtfeger and R. Schäfer, *Phys. Chem. Chem. Phys.*, 2014, **16**, 23952–23966.
12 T. M. Fuchs, F. Rivic and R. Schäfer, *Phys. Rev. A*, 2021, **104**, 012820.
13 S. Heiles, S. Schäfer and R. Schäfer, *J. Chem. Phys.*, 2011, **135**, 034303.
14 J. Bulthuis, J. A. Becker, R. Moro and V. V. Kresin, *J. Chem. Phys.*, 2008, **129**, 024101.
15 M. Schnell, C. Herwig and J. A. Becker, *Z. Phys. Chem.*, 2003, **217**, 1003–1030.
16 K. Jackson and J. Jellinek, *J. Chem. Phys.*, 2016, **145**, 244302.
17 J. P. Perdew, K. Burke and M. Ernzerhof, *Phys. Rev. Lett.*, 1996, **77**, 3865–3868.
18 D. E. Woon and T. H. Dunning, *J. Chem. Phys.*, 1992, **98**, 1358–1371.
19 A. Lehr, F. Rivic, M. Jäger, M. Gleditzsch and R. Schäfer, *Phys. Chem. Chem. Phys.*, 2022, **24**, 11616–11635.
20 A. Lehr, M. Jäger, M. Gleditzsch, F. Rivic and R. Schäfer, *J. Phys. Chem. Lett.*, 2020, **11**, 7827–7831.
21 M. Abd El Rahim, R. Antoine, M. Broyer, D. Rayane and P. Dugourd, *J. Phys. Chem. A*, 2005, **109**, 8507–8514.

22 R. S. Mulliken, *J. Chem. Phys.*, 1955, **23**, 1833–1840.
23 F. Martin and H. Zipse, *J. Comput. Chem.*, 2005, **26**, 97–105.
24 W. Parrish, *Acta Crystallogr.*, 1960, **13**, 838–850.
25 D. Wu, X. Wu, X. Liang, R. Shi, Z. Li, X. Huang and J. Zhao, *J. Phys. Chem. C*, 2018, **122**, 11086–11095.
26 S. Heydariyan, M. R. Nouri, M. Alaei, Z. Allahyari and T. A. Niehaus, *J. Chem. Phys.*, 2018, **149**, 074313.
27 S. Yoo, N. Shao and X. C. Zeng, *J. Chem. Phys.*, 2008, **128**, 104316.
28 W.-C. Lu, C. Z. Wang, L.-Z. Zhao, W. Zhang, W. Qin and K. M. Ho, *Phys. Chem. Chem. Phys.*, 2010, **12**, 8551–8556.
29 L. J. Lewis, *J. Non. Cryst. Solids*, 2022, **580**, 121383.
30 M. Khalkhali, Q. Liu, H. Zeng and H. Zhang, *Sci. Rep.*, 2015, **5**, 14267.
31 L.-s Li and A. P. Alivisatos, *Phys. Rev. Lett.*, 2003, **90**, 097402.
32 T. Nann and J. Schneider, *Chem. Phys. Lett.*, 2004, **384**, 150–152.
33 M. Shim and P. Guyot-Sionnest, *J. Chem. Phys.*, 1999, **111**, 6955–6964.
34 S. Shanbhag and N. A. Kotov, *J. Phys. Chem. B*, 2006, **110**, 12211–12217.
35 K. S. Cho, D. V. Talapin, W. Gaschler and C. B. Murray, *J. Am. Chem. Soc.*, 2005, **127**, 7140–7147.
36 Q. Zhao, L. Xie and H. J. Kulik, *J. Phys. Chem. C*, 2015, **119**, 23238–23249.
37 F. Jardali, B. P. Keary, T. Perrotin, F. Silva, J. C. Vanel, Y. Bonnassieux, S. Mazouffre, A. A. Ruth, M. E. Leulmi and H. Vach, *ACS Appl. Nano Mater.*, 2021, **4**, 12250–12260.

 